

# Centrality dependent long-range angular correlations of intermediate- $p_T$ D-mesons and charged particles in $pPb$ collisions at the LHC energy

Somnath Kar,<sup>1</sup> Subikash Choudhury,<sup>2</sup> Samrangy Sadhu,<sup>3</sup> and Premomoy Ghosh<sup>3,\*</sup>

<sup>1</sup>Key Laboratory of Quark and Lepton Physics (MOE) and Institute of Particle Physics, Central China Normal University, Wuhan 430079, China

<sup>2</sup>Key Laboratory of Nuclear Physics and Ion-beam Application (MOE) and Institute of Modern Physics, Fudan University, Shanghai 200433, China

<sup>3</sup>Variable Energy Cyclotron Centre, HBNI, 1/AF Bidhan Nagar, Kolkata 700 064, India

The high-multiplicity events of  $pPb$  collisions at  $\sqrt{s_{NN}} = 5.02$  TeV at the LHC exhibit unforeseen collective behaviour. One of the possible explanations to the collectivity could be the formation of thermalized partonic matter, like the one formed in relativistic nucleus-nucleus collisions and is described by the hydrodynamic models. This article presents a study on the centrality dependent long-range two-particle azimuthal correlations of D-mesons and charged particles in  $pPb$  collisions at  $\sqrt{s_{NN}} = 5.02$  TeV. The study has been conducted on the events, generated with the EPOS3 hydrodynamic code that reproduces most of the features of the  $pPb$  data at the LHC energy. There appears a ridge-like structure in the long-range two-particle angular correlations of D-mesons, in the intermediate  $p_T$ -range, and charged particles in the simulated high-multiplicity  $pPb$  events.

## I. INTRODUCTION

The thermalized partonic matter, the Quark-Gluon Plasma (QGP) [1, 2], has been observed in experiments [3–6] of ultra-relativistic gold-gold ( $AuAu$ ) collisions at the centre-of-mass energy ( $\sqrt{s_{NN}}$ ) of 130 and 200 GeV at the Relativistic Heavy Ion Collider (RHIC) at the BNL. Prior to the discovery at the RHIC, there had been efforts in search of the QGP in relativistic heavy-ion collisions at lower [7, 8]  $\sqrt{s_{NN}}$  and even in proton-proton ( $pp$ ) [9–11] collisions. Lack of confirmative signals for the QGP in the lower energy data pushed the requirement of the energy of collisions continually upwards. On the other hand, the relativistic heavy-ion collisions, considered to be more conducive to the QGP-thermalization because of the larger volume, longer lifetime and involvement of large number of nucleons, became the system of choice in search of the QGP. In extracting the signals of the QGP in the relativistic nucleus-nucleus collisions, the proton-proton and proton-nucleus collisions, however, play the role of the base-lines. Of the most significant features observed in the RHIC data, the collective flow of the final state particles produced in the collisions indicates thermalization and the suppression of the high- $p_T$  particles or the jets points to the formation of dense partonic medium. To derive the true medium effect on high- $p_T$  suppression, the heavy-ion data is studied in terms of the nuclear modification factor,  $R_{AA}$  [12], defined as the ratio of the yields in heavy-ion and  $pp$  collisions at the same energy in a given  $p_T$ -bin, normalized with the number of binary nucleon-nucleon collisions. The effect of the hot nuclear matter or

the QGP formed in heavy-ion collisions is finally estimated by disentangling the cold nuclear matter (CNM) effects [13–15], experimentally obtained from the proton-nucleus collisions. At the RHIC, however, the CNM effect was studied with deuteron-gold ( $dAu$ ) collisions because of technical difficulties for  $pAu$  collisions.

The Large Hadron Collider (LHC) has extended the domain of the QGP study. The heavy-ion program at the LHC experiments with heavier nuclei ( $PbPb$ ) and at higher  $\sqrt{s_{NN}}$  (2.76 and 5.02 TeV), create hotter partonic matter with increased energy density, volume and the lifetime [16]. It also facilitates the study of properties of the medium with copiously produced unique hard probes, the heavy-flavor (HF) particles. The LHC-data also indicate the possibility of formation of the QGP-like collective medium in small systems produced in the high multiplicity events of  $pp$  [17–20] and  $pPb$  [21–24] collisions. The recent analysis [25] of RHIC data on  $dAu$  collisions also corroborate the LHC finding. Though the source of the collectivity in the small systems is not yet unambiguously identified, there has been considerable effort in connecting the novel phenomenon with the QGP-like collectivity. Beside revealing [21–24] the long-range two-particle azimuthal angle correlations between charged particles, indicating collectivity in high-multiplicity events of  $pPb$  collisions at  $\sqrt{s_{NN}} = 5.02$  TeV, ALICE has studied [26] minimum-bias  $pPb$  data in terms of two-particle azimuthal correlations between the D-mesons and charged particles, in the short-range ( $|\Delta\eta| < 1$ , where  $\eta = -\ln \tan \theta/2$ , the pseudorapidity of a particle and  $\theta$  is the polar angle of the particle with respect to the beam direction). The study reports description of data by the EPOS3 generated events. In this article, we present a multiplicity dependent study of

---

\*Electronic address: prem@vecc.gov.in

simulated  $pPb$  events at  $\sqrt{s_{NN}} = 5.02$  TeV in terms of the two-particle azimuthal correlations between the D-mesons and charged particles, in the long-range ( $2 < |\Delta\eta| < 4$ ). The analysis has been carried out with the  $pPb$  events at  $\sqrt{s_{NN}} = 5.02$  TeV, generated by the EPOS 3 hydrodynamic model [27], that satisfactorily describes the features of collective behaviour of particle production in  $pPb$  events at the LHC.

## II. HEAVY-FLAVOR MESONS: THE PROBE

Because of the large masses, the production of HF-quarks (charm and bottom) predominantly takes place in the hard scattering of partons during the primordial stage of ultra-relativistic heavy-ion collisions. Most of the heavy quarks, produced in the heavy-ion collisions, thus witness the entire evolution of the QGP medium. Also, due to the large momentum transfer in the hard partonic interactions, the production cross-sections of heavy-quarks are calculable in the perturbative QCD approach. While diffusing through the medium, made of the light quarks and gluons, the heavy quarks experience radiative and collisional energy loss that is reflected in the spectra of the final state HF-mesons. The HF-meson (particularly the D-meson) has already played a significant role in characterising the medium formed in  $AuAu$  collisions [28–30] at RHIC as well as in  $PbPb$  [31, 32] and  $pPb$  [33] collisions at the LHC energies. The high  $p_T$  charm suppression has been observed in the central  $AuAu$  [28] and  $PbPb$  [31] collisions. The flow of charm has also been measured [29, 30] in the  $AuAu$  collisions at RHIC, in terms of the semi-leptonic decayed electrons. The D-mesons have been found to have medium induced collective flow [32] in the  $PbPb$  collisions at  $\sqrt{s_{NN}} = 2.76$  TeV. The ALICE has measured the nuclear modification factor,  $R_{pPb}$ , for D-mesons yields [33] and the relative yields of D-mesons as a function of relative charged particle multiplicity [34] in  $pPb$  collisions at  $\sqrt{s_{NN}} = 5.02$  TeV. The  $R_{pPb}$  measurement [33], revealing very small CNM effects for  $p_T \geq 3$  GeV/c, confirmed that the suppression of high  $p_T$  ( $\geq 2$  GeV/c) D-mesons [31] in  $PbPb$  collisions at  $\sqrt{s_{NN}} = 2.76$  TeV is predominantly due to final-state effect of the charm energy loss in the medium and not due to the initial-state CNM effect.

The “ridge” structure in high-multiplicity events of  $pPb$  collisions [21–24], as observed in two-particle correlation study with the light-flavored particles has been suggested to be due to either collectivity [35] or the gluon saturation [36]. Though, the collectivity in the high-multiplicity  $pPb$  events at the LHC energy is largely accepted, this study of long range azimuthal correlations of HF-mesons and charged particles in high-multiplicity  $pPb$  events could shed further light,

in this context.

## III. TWO-PARTICLE ANGULAR CORRELATIONS: THE ANALYSIS TOOL

The two-particle angular correlation function is defined by the per-trigger associated yields of charged particles obtained from  $\Delta\eta, \Delta\varphi$  distribution (where  $\Delta\eta$  and  $\Delta\varphi$  are the differences in the pseudo-rapidity ( $\eta$ ) and azimuthal angle ( $\varphi$ ) of the two particles) and is given by:

$$\frac{1}{N_{trig}} \frac{d^2 N^{assoc}}{d\Delta\eta d\Delta\varphi} = B(0, 0) \times \frac{S(\Delta\eta, \Delta\varphi)}{B(\Delta\eta, \Delta\varphi)} \quad (1)$$

where  $N_{trig}$  is the number of trigger particles in the specified  $p_T^{trigger}$  range.

The function  $S(\Delta\eta, \Delta\varphi)$  is the differential measure of per-trigger distribution of associated hadrons in the same-event, i.e.,

$$S(\Delta\eta, \Delta\varphi) = \frac{1}{N_{trig}} \frac{d^2 N_{same}^{assoc}}{d\Delta\eta d\Delta\varphi} \quad (2)$$

The same-event distribution functions are corrected for the random combinatorial background and effects due to the limited acceptance by dividing the raw same-event distribution function by the mixed-event background distribution, where trigger and associated particles are paired from two different events of similar multiplicity.

The background distribution function  $B(\Delta\eta, \Delta\varphi)$  is defined as:

$$B(\Delta\eta, \Delta\varphi) = \frac{d^2 N^{mixed}}{d\Delta\eta d\Delta\varphi} \quad (3)$$

where  $N^{mixed}$  is the number of mixed event pairs.

The factor  $B(0,0)$  in Eqn. 1 is used to normalize the mixed-event correlation function such that it is unity at  $(\Delta\eta, \Delta\varphi) = (0,0)$ . Finally, the acceptance corrected correlation function is determined by scaling the same-event distribution function,  $S(\Delta\eta, \Delta\varphi)$  by the inverse of the normalized background distribution function,  $B(\Delta\eta, \Delta\varphi)/B(0,0)$ .

The two-particle azimuthal correlations is a versatile analysis tool that addresses several sources of correlations in multiparticle production, depending on the studied ranges of  $|\Delta\eta|$  and also the  $p_T$  for the trigger and the associated particles. The “short-range”

( $|\Delta\eta| \sim 0$ ) two-particle azimuthal angle correlations are dominated by jets, produced in the hard QCD scattering. As the jets are produced back-to-back in azimuth, the jet correlations are reflected in the  $|\Delta\varphi|$  - distribution. The jet-induced per trigger hadron-pair yields from the same jet populate in the “near-side” at  $|\Delta\varphi| = (|\varphi_{trigger} - \varphi_{assoc.}|) \sim 0$ . The pair yields from the “away-side” jets show up at  $|\Delta\varphi| = (|\varphi_{trigger} - \varphi_{assoc.}|) \sim \pi$ . On the other hand, a ridge-like structure that appears in the “long-range” ( $|\Delta\eta| \gg 0$ ) two-particle azimuthal angle correlations in relativistic heavy-ion collisions, is attributed to the formation of a collective medium of particle production. The per trigger pair yields with small  $|\Delta\varphi|$  over a wide range of  $|\Delta\eta|$  (long-range), resulting a “ridge” structure also appears in the high multiplicity  $pp$  [17–20] and  $pPb$  [21–23] events at the LHC. The away-side signal of the long-range correlations contains contributions from jet-like correlations also, making it difficult to extract pure signal for long-range correlations. In search of collective medium of particle production, it is the near-side “long-range” or the “ridge-like” correlations, that becomes important as the near-side structure of the two-particle azimuthal angle correlations in the long-range is considered to be free from other effects.

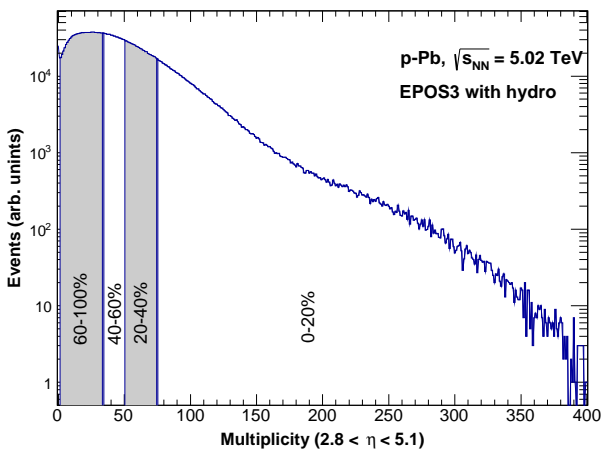


FIG. 1: Centrality selection for the EPOS3 generated events from the V0A acceptance [39] of ALICE set-up.

## IV. ANALYSIS AND RESULTS

### A. Event Generation by EPOS3

The EPOS3 is a hybrid MC event generator having three basic ingredients, a flux-tube initial condition, 3+1D viscous hydrodynamics and a

hadronic afterburner modelled via UrQMD. In addition, it implements interplay between hard and soft physics processes. The most important aspect of the EPOS3 simulation code for particle production at the LHC energy is probably the similar treatment adopted in *proton – proton*, *proton – nucleus* and *nucleus – nucleus* collisions, which facilitate understanding the observed feature of collectivity in the high-multiplicity  $pp$  and  $pPb$  events at the LHC vis-a-vis the exhaustively studied collective phenomena in relativistic *nucleus – nucleus* collisions.

In this model, an elementary scattering of partons give rise to parton ladder. Each parton ladder is considered as a longitudinal color field or a flux tubes, carrying transverse momentum of the hard scattering. The flux tubes expand and at some stage get fragmented into string segments of quark-antiquark pairs. In case of many elementary parton-parton scattering in an event of ultra-relativistic  $pp$ ,  $p – nucleus$  or *nucleus – nucleus* collisions, resulting high-multiplicity, a large number of flux tubes are produced, eventually leading to high local string-segment density. The high energy of string segments and / or high local string-segment density (above a critical value) constitute the bulk matter, forming the medium. The string segments in the bulk matter, which do not have enough energy to escape, form a “core” of thermalized “plasma” that undergoes hydrodynamical expansion following (3 + 1D) viscous hydrodynamic evolution followed by Cooper-Frye mechanisms of particle production. After that, the hadronic evolution takes place till the freeze-out of the “soft” (low  $p_T$ ) hadrons. On the other hand, the “hard” particles or the “high”  $p_T$  jet-hadrons originate from hadronization by Schwinger’s mechanism of the high-energy string segments from the “corona”, the less dense medium in the periphery of the bulk-matter. The “semi-hard” or the “intermediate- $p_T$ -range particles originate from the string-segments with enough energy to escape the bulk-matter. These string-segments, while escaping from within the bulk-matter, may pick-up quark-antiquark from the medium. As a result, the intermediate- $p_T$  particles inherits the properties of the bulk medium.

According to the initial conditions of the EPOS3, the heavy quarks may be produced [38] in the initial stage, whenever the massive quark - antiquark production is possible, through fragmentation of flux tubes or the parton ladders, formed in elementary scattering of partons. In multiple scattering in the EPOS framework, many parton ladders are produced, while each of the parton ladders contributes in production of the charm as well as the light quarks leading to the production of D-mesons and light hadrons. Although no interaction between the heavy quarks and the bulk thermalized

matter is implemented [38] in EPOS3, the majority of the particles in the “intermediate”  $p_T$ -range in the EPOS framework, which come from the semi-hard string fragmentations, carry the property of the bulk matter and also enough energy to escape it. So, the D-mesons originating from the initial semi-hard processes in the intermediate  $p_T$ -range also are likely to reflect the collective property of the bulk fluid, like the other light hadrons. With these considerations, to explore the collective nature of the high-multiplicity  $pPb$  events at the LHC energy in terms of the long-range two particle angular correlations of the D-mesons, in the intermediate  $p_T$ -range, and the charged particles, we have generated 18 million minimum-bias  $pPb$  events at  $\sqrt{s_{NN}} = 5.02$  TeV, using the EPOS3.107 code.

To make this centrality-dependent study of the simulated events more like data analysis by the experiments, for the centrality estimation, we follow the technique, identical to the one followed by the ALICE. Also, we validate the generated events by reproducing the available centrality-dependent ALICE measurements which are relevant to the type of analysis we aim to carry out.

## B. Centrality Estimation

In ALICE, the event classes are obtained either from the signal amplitude in the VZERO detector in the forward / backward rapidity region ( $2.8 < \eta < 5.1$ ) or from the reconstructed tracklets from the Silicon Pixel Detector (SPD) in the mid-rapidity  $|\eta| < 1.0$ , in the ALICE experimental set-up. For the centrality estimation from the VZERO detector, the minimum-bias events are divided into several event classes, defined as fraction of the analyzed event sample, based on the cuts on the total deposited charge in the VZERO detector in the Pb-going direction. The deposited charge on the VZERO detector is proportional to the multiplicity of the charged particle in the covered pseudo-rapidity interval. The ALICE measurements show [39] that the deposited charge on the VZERO detector or equivalently the mean charge particle multiplicity is proportional to the centrality of events. For this analysis with the simulated events, for the centrality selection, we consider the charged particle multiplicity in the lead-going direction in the pseudo-rapidity region of  $2.8 < \eta < 5.1$ , which is the acceptance of the respective VZERO detector in the ALICE set-up. We take into account the asymmetric  $pPb$  collisions, where the *nucleon – nucleon* center-of-mass system moves in the direction of the proton beam corresponding to a rapidity of  $y_{NN} = -0.465$ , resulting the laboratory reference interval  $|y_{lab}| < 0.5$  shifting of the centre-of-mass rapidity coverage of  $-0.96 < y_{cms} < 0.04$ . In Figure 1, we have shown the fractions of

multiplicity distributions as the centrality selection for the EPOS3 generated minimum-bias events.

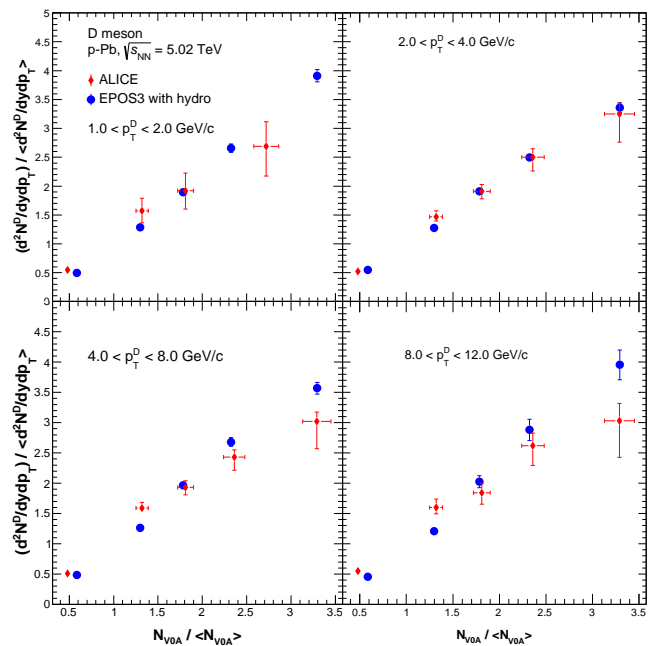


FIG. 2: Relative D-meson yields as a function of charged particle multiplicity for the  $p_T$  ranges 1-2, 2 - 4, 4 - 8 and 8 - 12 GeV/c in  $pPb$  collisions at  $\sqrt{s_{NN}} = 5.02$  TeV, measured by the ALICE, are compared with the EPOS3 generated events.

## C. Validation of generated event-sample

### 1. Relative yields of D-meson as a function of relative charged particle multiplicity

The ALICE measurement [34] of average relative yields of D-mesons,  $(d^2N_D/dydp_T) / \langle d^2N_D/dydp_T \rangle$  as a function of relative yields of charged particle multiplicity  $(dN_{ch}/d\eta) / \langle dN_{ch}/d\eta \rangle$  for different  $p_T$  bins have been reported [34] to be well reproduced by EPOS3. To validate our generated events to continue with further studies as a function of charged particle multiplicity, we calculate relative yields of D-meson as a function of relative yields of charged particle,  $N_{V0A} / \langle N_{V0A} \rangle$ , estimated from the pseudorapidity coverage of the acceptance of the VZERO detector of ALICE experiment. In Figure 2, we present the centrality or equivalently the multiplicity dependence of relative D-mesons yields for four  $p_T$ -bins, 1 to 2, 2 to 4, 4 to 8 and 8 to 12 GeV/c, as obtained from the EPOS3 generated events along with those measured

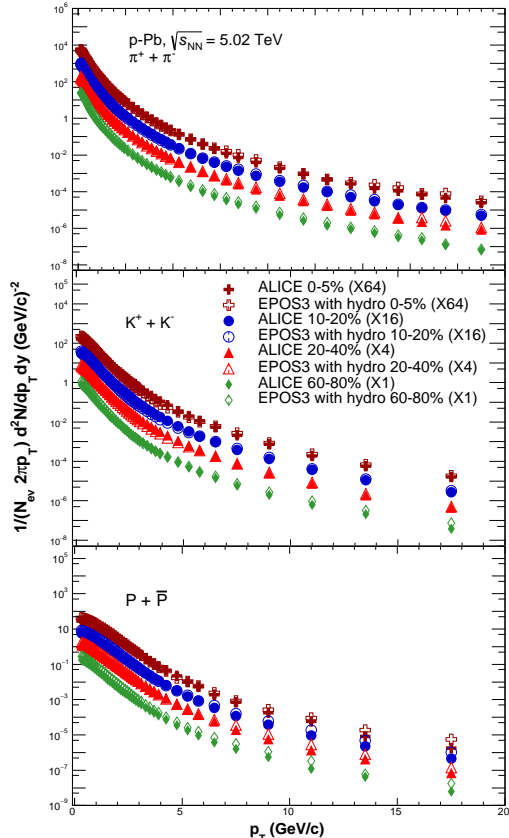


FIG. 3: Centrality dependent invariant yields of identified charged particles in  $pPb$  collisions at  $\sqrt{s_{NN}} = 5.02$  TeV, measured by ALICE [37], are compared with the simulated events from the EPOS3 event generator.

by the ALICE. The simulated events reasonably reproduces the measured multiplicity dependence of relative D-meson yields in  $pPb$  collisions at  $\sqrt{s_{NN}} = 5.02$  TeV.

## 2. Centrality dependent invariant yields of identified charged particles

Having the generated events validated by matching the relative D-mesons yields, as measured by ALICE, as a function of relative charged particle multiplicity, it will be relevant to see how the generated events describe the measured multiplicity dependent yields of the identified charged particles. The ALICE has measured [37, 40] invariant yields of identified charged particles,  $\pi^\pm$ ,  $K^\pm$  and  $p$ ,  $\bar{p}$  for different centrality classes of events. We obtain the invariant yield spectra for the identified charged particles, for the chosen centrality classes, from the EPOS3 generated events and plot the spectra in Figure 3, along with the

respective spectra measured by ALICE.

It may be noted that, for comparing with the ALICE data, we have used same scale-factors while plotting the calculated yields in the Figure 3 and because of the chosen scale, to accommodate all in one figure, the goodness of the description of the data with the EPOS3 calculations is not clear on visual inspection. Further investigation in terms of ratio, (EPOS3 Calculation)/(ALICE Data), reveals that, on an average, the EPOS3 calculated yields of intermediate- $p_T$  charged particles lie within about 20 % of the ALICE data for the top three of the considered centrality classes. For the event-class of 60-80 % centrality, the deviation is larger. These calculations are consistent with the previous EPOS3 calculations [27] on invariant yields of identified particles in  $pPb$  collisions.

Our EPOS3-generated event-sample thus reasonably reproduces the multiplicity dependent yields for D-meson and identified charged particles in  $pPb$  collisions at  $\sqrt{s_{NN}} = 5.02$  TeV, at least for central events, and the results of calculations are consistent with those of previous EPOS3 calculations [27, 34]. Validating the generated event-sample, we now proceed to study the long-range azimuthal correlations between D-mesons and charged particles in high-multiplicity  $pPb$  events.

## D. Long-range ridge-like correlations

In case of formation of collective medium, the long-range two-particle angular correlations of “soft” particles ideally exist over the entire  $|\Delta\eta|$ -range. The effect, however, gets submerged by the dominant jet-like correlation in the short-range ( $|\Delta\eta| \sim 0$ ). On the other hand, the ridge-like, bulk correlations appear prominent in the long  $|\Delta\eta|$ -range, ( $|\Delta\eta| \gg 0$ ) where jet-like short-range correlations are almost absent. At the LHC, ALICE, CMS and ATLAS have studied [21–23] the centrality dependent long-range two-particle correlations of charged particles in  $pPb$  collisions at  $\sqrt{s_{NN}} = 5.02$  TeV. In this work, for the centrality dependent long-range, D-mesons charged particles angular correlations study with the simulated events, we choose the same  $|\Delta\eta|$ -range and similar  $p_T$ -ranges (to start with), as used by the CMS experiment in revealing [22] the ridge-like structure in the near-side long-range azimuthal correlations for charged particles in the  $pPb$  data at  $\sqrt{s_{NN}} = 5.02$  TeV. This helps us to qualitatively compare our study with existing results from similar analysis, in terms of the  $\Delta\varphi$  distributions of the per trigger yields.

So, for the study of the D-mesons and charged particles angular correlations in the long-range, we

consider  $2 < |\Delta\eta| < 4$ . The CMS experiment has studied multiplicity ( $N_{track}$ ) - dependent near-side, long-range angular correlations for charged particles in  $pPb$  collisions at  $\sqrt{s_{NN}} = 5.02$  TeV in different  $p_T$ -intervals, 0.1 to 1, 1 to 2, 2 to 3 and 3 to 4 GeV/c, with the same  $p_T$ -ranges for both the triggers and the associated particles. The study revealed most prominent ridge-like structure in the high-multiplicity events in the 1 to 2 GeV/c  $p_T$ -interval. The ridge-like structure diminishes with higher  $p_T$  and nearly disappears in the  $p_T$ -interval 3 to 4 GeV/c.

We first construct the long-range two-particle azimuthal correlations for the hadrons and the charged particles in the simulated events for the same centrality classes as estimated and described in the beginning of this article for the  $p_T$ -intervals 1 to 2, 2 to 3 and 3 to 4 GeV/c. The per trigger correlated yield, projected onto  $\Delta\varphi$  and subtracted by the  $Yield|_{\Delta\varphi=1.0}$  (the per trigger correlated yield at  $\Delta\varphi = 1.0$ ) for  $2 < |\Delta\eta| < 4$  for different centrality bins are obtained and shown in the Figure 4. The centrality dependence of the correlated yield as a function of  $\Delta\varphi$  for different  $p_T$ -intervals in the simulated events reveals similar feature as observed in the two-particle azimuthal correlations of the charged particles with the CMS data [22]: the ridge-like structure is most prominent in the 1 to 2 GeV/c  $p_T$ -range and in the most central events, while it gradually decreases with increasing  $p_T$ .

Next, the long-range two-particle azimuthal correlations are constructed for D-mesons and charged particles from the simulated events for the same centrality classes and in the same  $p_T$ -intervals 1 to 2, 2 to 3 and 3 to 4 GeV/c. The per trigger correlated yields, in the long-range, are projected onto  $\Delta\varphi$  for different centrality bins. The  $\Delta\varphi$  distributions are plotted in the figure 5. As depicted in the figure 5, the centrality dependence the correlated yield as a function of  $\Delta\varphi$  for the different  $p_T$ -intervals in the simulated events in the considered  $p_T$  intervals do not really show the features as observed in case of two-particle correlations of hadrons and charged particles. The non-appearance of the ridge-like structure in the ‘‘low’’  $p_T$ -range appears consistent in view of the production of the heavy-quarks and their non-interaction with the thermalized bulk-matter in the EPOS3 framework.

At this point, we recollect that ALICE has measured [32] significant positive  $v_2$  (comparable in magnitude to the light-flavored charged hadrons  $v_2$ ) of the D-mesons in the  $2 < p_T < 6$  GeV/c range, in 30 - 50 % centrality class of  $PbPb$  collisions at  $\sqrt{s_{NN}} = 2.76$  TeV. The ALICE result and the fact that the measured  $v_2$  of light charged particles at RHIC and LHC are usually observed to have the positive  $v_2$  up to the  $p_T$ -range of about 3 GeV/c, prompt us to consider respective

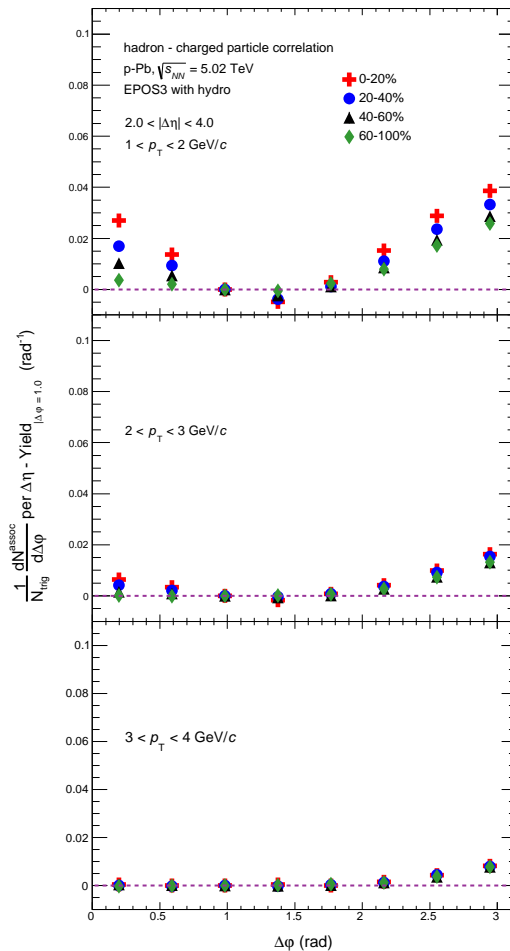


FIG. 4: Centrality dependent correlated yield as a function  $\Delta\varphi$  and subtracted by the  $Yield|_{\Delta\varphi=1.0}$ , as obtained from the long-range two-particle azimuthal correlations of hadrons (as triggered particles) and charged particles, averaged over  $2 < |\Delta\eta| < 4$ , for EPOS3 generated  $pPb$  collisions at  $\sqrt{s_{NN}} = 5.02$  TeV in different ranges of the same  $p_T^{trigger}$  and  $p_T^{associated}$ .

$p_T$ -ranges for D-mesons and the charged particles for studying collectivity in terms of the long-range two-particle angular correlations. Incidentally and also importantly, as argued in the Section - IV.A, the D-mesons in the intermediate  $p_T$ -range, in the hydrodynamic-EPOS3 approach, inherently carry the collective property of the bulk fluid. It may also be noted that the modulations in the  $\Delta\varphi$  distributions of the two-particle angular correlations actually represent the cumulative effects due to the  $v_2$  and its higher harmonics which, for the long-range correlations, can be factorized as the  $v_n(p_T^{trigger})v_n(p_T^{associated})$ . We construct the long-range two-particle azimuthal correlations for the D-mesons and the charged particles for  $2 < |\Delta\eta| < 4$ ,  $3 < p_T^{trigger} < 5$  GeV/c and  $1 < p_T^{associated} < 3$  GeV/c from 18 million simulated events in the selected

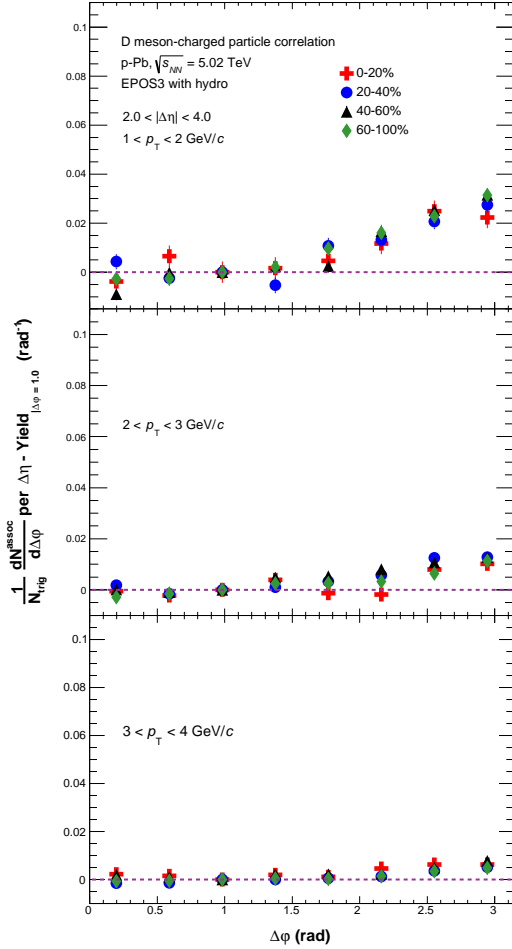


FIG. 5: Centrality dependent correlated yield as a function  $\Delta\varphi$  and subtracted by the  $Yield_{|\Delta\varphi|=1.0}$ , as obtained from the long-range two-particle azimuthal correlations of D-mesons (as triggered particles) and charged particles, averaged over  $2 < |\Delta\eta| < 4$ , for EPOS3 generated  $pPb$  collisions at  $\sqrt{s_{NN}} = 5.02$  TeV in different ranges of the same  $p_T^{trigger}$  and  $p_T^{associated}$ .

centralities. In the considered  $p_T$ -ranges, the long-range two-particle azimuthal correlations of D-mesons and charged particles indeed reveal a prominent ridge-like structure in the most central event-class, as has been depicted in Figure 6 and Figure 7, after removing the short-range jet-like correlations. To compare with the EPOS3 generated events without hydrodynamic evolution we repeat the correlation study on similar statistics of EPOS3 generated non-hydro events. The ridge-like structure does not appear for EPOS3 generated high-multiplicity  $pPb$  events at  $\sqrt{s_{NN}} = 5.02$  TeV, without non-hydrodynamic evolution, as expected. At this stage, we like to point out that negative values of the correlations which appear in the near-side for the 40 - 60 % and 60 - 100 % centrality classes (Figure 7) have no physics origin and these

D meson-charged particle correlation  $3 < p_T^{trig} < 5$  GeV/c  
 p-Pb,  $\sqrt{s_{NN}} = 5.02$  TeV, EPOS3 with hydro  $1 < p_T^{assoc} < 3$  GeV/c

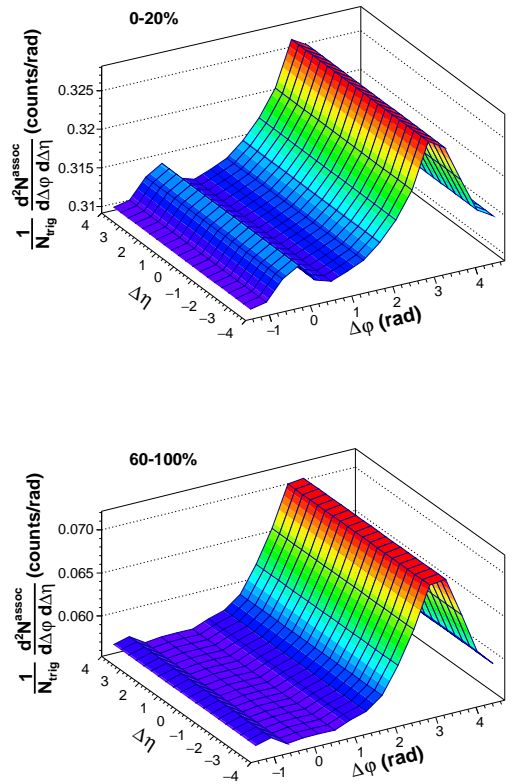


FIG. 6: Two particle  $\Delta\eta - \Delta\varphi$  correlation function for  $3 < p_T^{trigger} < 5$  GeV/c and  $1 < p_T^{associated} < 3$  GeV/c with D-meson as trigger particles for the hydrodynamic-EPOS3 generated  $pPb$  collisions at  $\sqrt{s_{NN}} = 5.02$  TeV in 0 - 20 and 60 - 100 per cent central event classes. The short-range correlations has been suppressed for conspicuous presentation of the long-range correlations.

result as an artefact of baseline subtraction. Since in peripheral collisions, long range region may have fluctuations due to few pairs in same event and mixed event which makes determination of baseline uncertain.

The appearance of the ridge-like structure in the long-range two-particle angular correlations of the D-mesons, in the intermediate  $p_T$ -range, and charged particles in the high-multiplicity EPOS3 generated  $pPb$  events reflects the collective property of the D-mesons. In view of identifying the source of the collective property of the, D-mesons in the EPOS framework, therefore, we investigate the generated events further. We select two different classes of D-mesons according to the production mechanisms: 1) "soft" particles from the "core" or the plasma and 2) the particles from semi-hard string fragmentation. We calculate the invariant yields separately for the two selected classes of generated particles. The figure 8 clearly shows that the

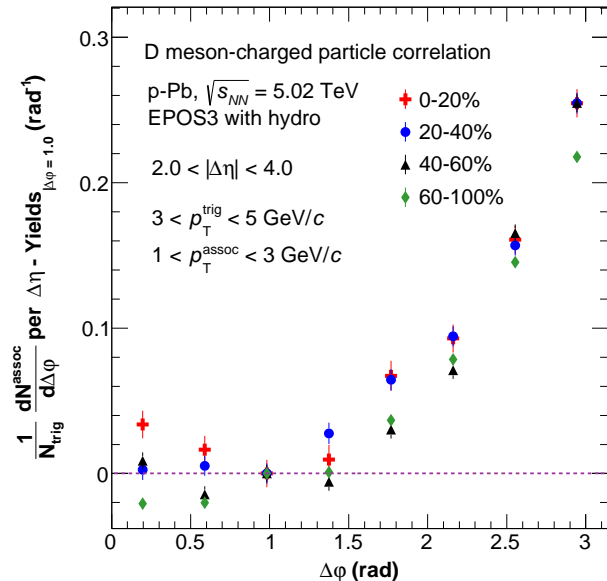


FIG. 7: Centrality dependent correlated yield as a function  $\Delta\varphi$  and subtracted by the  $Yield_{|\Delta\varphi=1.0}$ , as obtained from the long-range two-particle azimuthal correlations of D-mesons and charged particles, averaged over  $2 < |\Delta\eta| < 4$ , for  $3 < p_T^{trigger} < 5$  GeV/c and  $1 < p_T^{associated} < 3$  GeV/c for the hydrodynamic-EPOS3 generated  $pPb$  collisions at  $\sqrt{s_{NN}} = 5.02$  TeV.

D-meson yield from (semi-)hard string fragmentation (non-plasma source) dominate largely the same from the plasma source in EPOS3 hydrodynamic framework.

We calculate the long range two particle angular correlations, between D-mesons from different sources and the charged particles and plot the  $\Delta\eta - \Delta\varphi$  correlation function for  $3 < p_T^{trigger} < 5$  GeV/c and  $1 < p_T^{associated} < 3$  GeV/c with D-meson as trigger particles for the hydrodynamic-EPOS3 generated  $pPb$  collisions at  $\sqrt{s_{NN}} = 5.02$  TeV in 0 - 20 and 60 - 100 per cent central event classes, in figure 9 for a) the plasma source and b) the non-plasma source.

In the figure 10, we compare the centrality dependent per trigger correlated yield from the two sources as a function  $\Delta\varphi$  and subtracted by the  $Yield_{|\Delta\varphi=1.0}$ , as obtained from the long-range two-particle azimuthal correlations of D-mesons and charged particles, averaged over  $2 < |\Delta\eta| < 4$ , for  $3 < p_T^{trigger} < 5$  GeV/c and  $1 < p_T^{associated} < 3$  GeV/c for the hydrodynamic-EPOS3 generated  $pPb$  collisions at  $\sqrt{s_{NN}} = 5.02$  TeV. It becomes clear from the figure 10, that the per trigger two-particle correlated yield is more for the D-mesons from the plasma source than the one from the non-plasma source. However, as the yield of the D-mesons

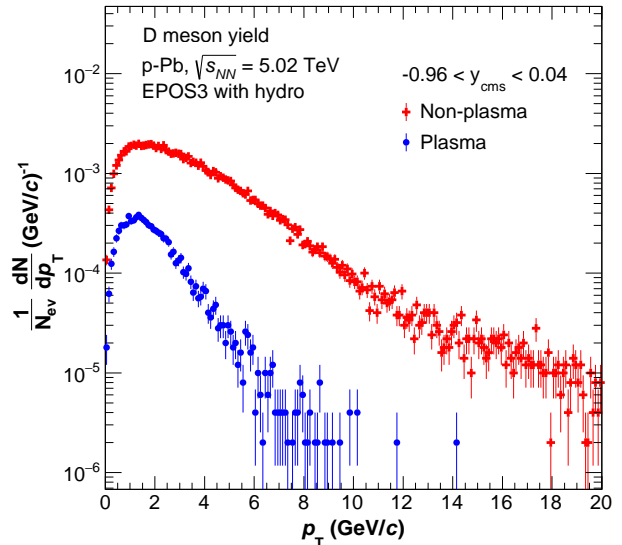


FIG. 8: Invariant yield of EPOS3 generated D-mesons from two different sources, plasma and non-plasma.

from the non-plasma source is much more than the yield of that from the plasma source, in order of magnitude, the relative contribution of the two sources in the overall per trigger yields become comparable.

At this stage, it will be pertinent to investigate how does the EPOS3 event generator describe the  $p_T$  - differential cross sections of D-mesons measured at the LHC. Our analysis reveals (figure 11) that the inclusive D-mesons yields match with the ALICE data [33] only in the high- $p_T$  region,  $p_T > 6$  GeV/c. On further investigation, we find that D-mesons from hard-scatterings or non-plasma has a reasonable agreement with data in the aforementioned region and also it is a dominant source of D-mesons production. We also note that D-mesons from non-plasma, like the inclusive D-mesons, fail to reproduce D-meson yield in  $p_T$  - range,  $p_T < 6$  GeV/c. On the other hand, D-mesons production from plasma (green open circle) is highly underestimated, though its spectral shape matches with that of the data. It may be noted that the D-meson yields from plasma in EPOS generated events have been scaled with an arbitrary number and depicted in the figure 11 to compare the spectral shape.

## V. SUMMARY AND DISCUSSIONS

We have studied the centrality or the multiplicity dependence of the long-range ( $2 < |\Delta\eta| < 4$ ) two-particle angular correlations for the D-mesons and charged particles, produced in EPOS3-generated  $pPb$

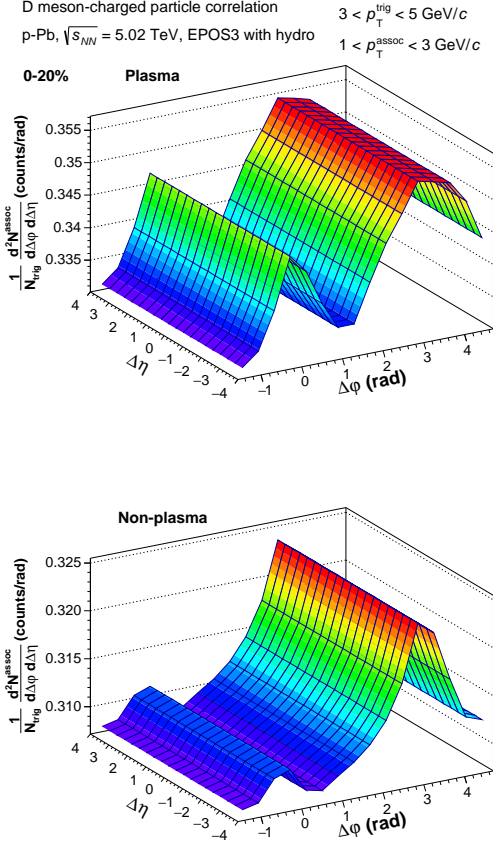


FIG. 9: Same as Figure 6 for D-mesons generated from the plasma (upper panel) and non-plasma (lower panel) sources for 0 - 20 per cent central event class.

events at  $\sqrt{s_{NN}} = 5.02$  TeV. This study with EPOS3 generated events is motivated with the observed [26] matching of EPOS3 events and the minimum-bias ALICE data of  $pPb$  collisions at  $\sqrt{s_{NN}} = 5.02$  TeV on the short-range two-particle correlations between D-mesons and charged particles.

The ridge-like structures as observed [22] in the  $pPb$  data in the study in two-particle angular correlations between charged particles, in the low  $p_T$ -range (most prominent in the  $p_T$  range 1 - 2 GeV/c) is absent in the angular correlations between the D-mesons and the charged particles, in the similar  $p_T$ -range, in the EPOS3 generated events. The observation appears to be in accordance with the EPOS3 code, in the present form, where interactions of heavy-quarks with the thermalized bulk matter is not implemented.

However, this study on the two-particle angular correlations of D-mesons in the intermediate  $p_T$ -range, ( $3 < p_T^{trigger} < 5$  GeV/c) and the charged particles in low- $p_T$  range,  $1 < p_T < 3$  GeV/c, of the EPOS3 generated

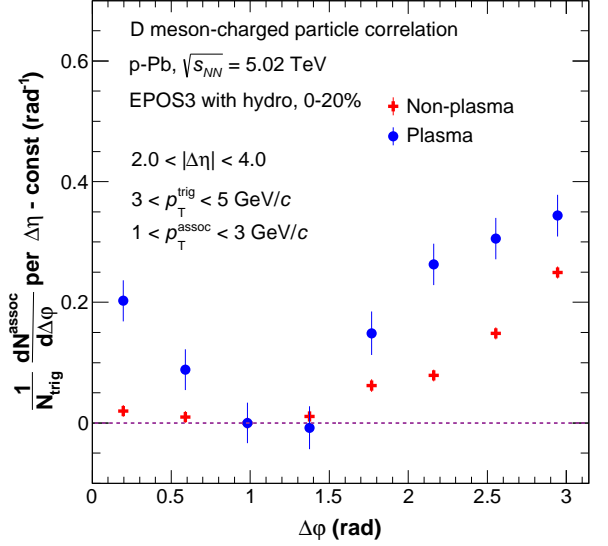


FIG. 10: Same as Figure 7 for generated particles from two separate sources, plasma and non-plasma.

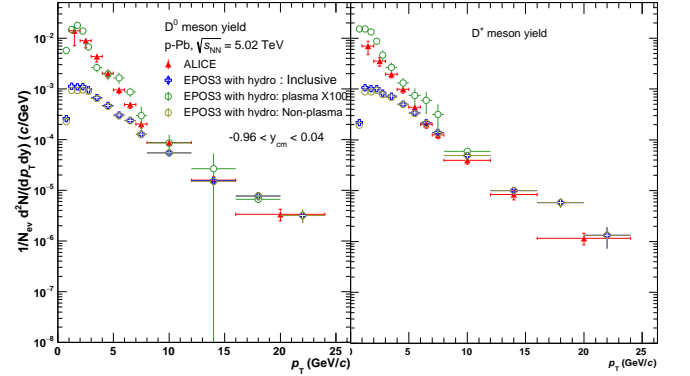


FIG. 11:  $p_T$  - differential cross sections of D-mesons in EPOS-hydro generated events, compared with data. The EPOS-yields from plasma is scaled with arbitrary factor to compare the the spectral shapes.

events clearly shows a prominent ridge-like structure in the long-range in high-multiplicity EPOS3-generated  $pPb$  events. According to the EPOS3 hydrodynamic model, high-multiplicity events are generated from large number of flux tubes created in many initial parton-parton scatterings in an event. A large number of flux-tubes breaks to form a medium of high string-segment density. The low- $p_T$  final state particles come from the thermalized bulk-matter created with low energy string-segments. The semi-hard particles, like the D-mesons in the intermediate  $p_T$ -range, ( $3 < p_T^{trigger} < 5$  GeV/c), having enough energy to escape the bulk-matter, hadronize by picking-up quark or

antiquark from the bulk-matter. The D-mesons in this intermediate  $p_T$ -range, thus carry the collective property of the bulk-matter, as reflected in the ridge-like structure in two-particle angular correlations between the D-mesons in this  $p_T$  range and charged particles in low- $p_T$  range. Further analysis (results depicted in figures 9 and 10), in terms of correlated pair yields per trigger, suggests that major contribution to the observed ridge-like structure indeed comes from the D-mesons produced in the bulk-matter or the “plasma”.

This study addresses the particular issue of formation of collective medium in high-multiplicity  $pPb$  collisions in ultra-relativistic collisions and its response to the heavy-flavour particles. The study of collectivity and search for its origin in the high-multiplicity  $pPb$  events attracted significant attention only after the unexpected experimental observations of collective behaviour in particle production in this small system [21–24] at the LHC energies. Moreover, even at the available LHC energies, the statistics of high-multiplicity events  $pPb$  collisions is not sufficient yet to study the properties of the small collective medium, exhaustively, in terms of all the possible probes, including heavy-flavour particles, the established [41, 42] hard-probe, considered to be very effective in characterization of the parton-medium interactions and of the properties of QGP, the strongly interacting matter that is formed [3–6] in ultra-relativistic heavy-ion collisions. At this stage, for understanding the collective property of particle production in high-multiplicity  $pPb$  collisions, simulation-based studies with well established event generator and comparison of  $pPb$  data with  $PbPb$  data play important roles. In the context of comparing collective property of PbPb and high-multiplicity pPb collisions, a very recent revelation [43] of an anti-correlation of  $v_2$  and  $v_3$  of similar strength for the charged particles in events of same multiplicity of  $pPb$  and  $PbPb$  data, by strengthening the idea of common origin of the collectivity, allows us to discuss existing similar studies, theoretical and experimental, on intermediate- $p_T$  heavy flavour particles in  $PbPb$  collisions. It is interesting to note that the collective behaviour of the intermediate  $p_T$  D-mesons from the EPOS3 generated  $pPb$  events at  $\sqrt{s_{NN}} = 5.02$  TeV is consistent with results from several studies on D-mesons in the similar  $p_T$ -range of  $PbPb$  collisions data at the LHC. In  $PbPb$  collisions at  $\sqrt{s_{NN}} = 2.76$  TeV the  $R_{AA}$  of D-mesons and light-flavour hadrons have been found [44] to be consistent for  $p_T > 6$  GeV/c whereas for  $p_T < 6$  GeV/c, the  $R_{AA}$  of D-mesons tends

to be slightly higher than that of pions. It is worth mentioning that a hybrid model [45] of fragmentation and coalescence, by incorporating nuclear shadowing effect in the initial state and including both the radiative and collisional energy loss of heavy quarks inside the QGP matter, can satisfactorily describe the D-meson  $R_{AA}$  in central  $PbPb$  collisions at  $\sqrt{s_{NN}} = 2.76$  TeV data [44]. The hybrid model calculations show that of the two hadronization processes of heavy quarks in the QGP medium, the fragmentation and the heavy-light quark coalescence, while the fragmentation dominates for  $p_T > 8$  GeV/c, the coalescence becomes crucial in explaining the data in intermediate and low  $p_T$ -ranges. Further on experimental results, it may be noted that the intermediate  $p_T$ -range of the D-meson, as considered in this study, falls within the  $p_T$ -range ( $2 < p_T < 6$  GeV/c) of the D-mesons in the  $PbPb$  collisions at  $\sqrt{s_{NN}} = 5.02$  TeV [32] which exhibit medium induced hydrodynamic collectivity in terms of positive  $v_2$ . In another recent study [46], the magnitude of the azimuthal anisotropy coefficients,  $v_2$  and  $v_3$  for the prompt  $D^0$ -mesons for  $p_T < 6$  GeV/c the  $PbPb$  collisions at  $\sqrt{s_{NN}} = 5.02$  TeV have been reported. In comparison to measurements for the charged particles, these measurements for the prompt  $D^0$ -meson have been found [46] to be smaller. As the momentum of the D-mesons, with constituent quarks of unequal masses, is mostly contributed by the heavy charm-quark, the constituent light-quark has to have low momentum and low  $v_2$  [47, 48], resulting slower development of collective features with the  $p_T$ .

Considering observed collective properties of D-mesons, in the intermediate  $p_T$ -range, in ultra-relativistic heavy-ion collisions and several similarities in features of particle production data of  $pPb$  and  $PbPb$  collisions, the prediction of collective behaviour of intermediate- $p_T$  D-mesons in the EPOS3 generated high-multiplicity  $pPb$  events, which reproduce other observations in  $pPb$  data, appears reliable.

## VI. ACKNOWLEDGEMENT

The authors are thankful to Klaus Werner for providing them with the EPOS3 code. SC acknowledges financial support from National Science Foundation of China.

---

[1] J. C. Collins and M. J. Perry, Phys. Rev. Lett. **34**, 1353 (1975).

[2] E. Shuryak, Phys. Rep. **61**, 71 (1980).

[3] I. Arsene et al., BRAHMS Collaboration, Nucl. Phys.

- A757**, 1 (2005).
- [4] B. B. Back et al., PHOBOS Collaboration, Nucl. Phys. **A757**, 28 (2005).
- [5] J. Adams et al., STAR Collaboration, Nucl. Phys. **A757**, 102 (2005).
- [6] K. Adcox et al., PHENIX Collaboration, Nucl. Phys. **A757**, 184 (2005).
- [7] S. J. Lindenbaum et al., AIP Conference Proceedings **176**, 778 (1988).
- [8] U. Heinz, M. Jacob, arXiv: nucl-th/0002042.
- [9] Richard M. Weiner, Int. J. Mod. Phys. E 15, 37 (2006).
- [10] P. Levai and B. Muller, Phys. Rev. Lett. **67** 1519 (1991).
- [11] T. Alexopoulos et al., Phys. Lett. **B528**, 43 (2002).
- [12] K. Adcox et al., PHENIX Collaboration, Phys. Rev. Lett. **88**, 022301 (2002).
- [13] J. W. Cronin et al., Phys. Rev. **D11**, 3105 (1975).
- [14] Nestor Armesto, J. Phys. G: Nucl. Part. Phys. **32**, R367 (2006).
- [15] Zhong-Bo Kang, Ivan Vitev, Hongxi Xing, Phys. Lett. **B718**, 482 (2012).
- [16] B. Muller, J. Schukraft, and B. Wyslouch, Annu. Rev. Nucl. Part. Sci. **62**, 361 (2012).
- [17] V. Khachatryan et al., CMS Collaboration, J. High Energy Phys. **09**, 091 (2010).
- [18] G. Aad et al., ATLAS Collaboration, Phys. Rev. Lett. **116**, 172301 (2016).
- [19] V. Khachatryan et al., CMS Collaboration, Phys. Rev. Lett. **116**, 172302 (2016).
- [20] V. Khachatryan et al., CMS Collaboration, Phys. Lett. **B765**, 193 (2017).
- [21] B. Ablev et al., ALICE Collaboration, Phys. Lett. **B719**, 29 (2013).
- [22] S. Chatrchyan et al., CMS Collaboration, Phys. Lett. **B718**, 795 (2013).
- [23] G. Aad et al., ATLAS Collaboration, Phys. Rev. Lett. **110**, 182302 (2013).
- [24] B. Ablev et al., ALICE Collaboration, Phys. Lett. **B728**, 25(2014).
- [25] A. Adare et al., PHENIX Collaboration, Phys. Rev. Lett. **114**, 192301(2015).
- [26] J. Adam et al., ALICE Collaboration, Euro. Phys. J. **C77**, 245 (2017).
- [27] K. Werner, et al., Phys. Rev. **C89**, 064903 (2014).
- [28] L. Adamczyk, et al. STAR Collaboration Phys. Rev. Lett. **113**, 142301 (2014).
- [29] A. Adare, et al. PHENIX Collaboration Phys. Rev. Lett. **98**, 172301 (2007).
- [30] L. Adamczyk et al. STAR Collaboration Phys. Rev. **C95**, 034907 (2017).
- [31] B. Abelev et al., ALICE Collaboration, J. High Energy Phys. **09**, 112 (2012).
- [32] B. Abelev et al., ALICE Collaboration, Phys. Rev. Lett. **111**, 102301 (2013).
- [33] B. Abelev et al., ALICE Collaboration, Phys. Rev. Lett. **113**, 232301 (2014).
- [34] B. Abelev et al., ALICE Collaboration, J. High Energy Phys. **08**, 078 (2016).
- [35] P. Bozek., Phys. Rev. **C85**, 014911 (2012).
- [36] K. Dusling and R. Venugopalan, Phys. Rev. **D87**, 094034 (2013).
- [37] J. Adam et al., ALICE Collaboration, Phys. Lett. **B760**, 720 (2016).
- [38] K. Werner et al., J. Phys. : Conf. Ser. 736 012009 (2016).
- [39] J. Adam et al., ALICE Collaboration, Phys. Rev **C91**, 064905 (2015).
- [40] <https://doi.org/10.17182/hepdata.73749>.
- [41] R. Averbeck, Prog. Part. Nucl. Phys. 70 159 (2013).
- [42] F. Prino and R. Rapp, J. Phys. G:Nucl. Part. Phys. 43 093002 (2016).
- [43] A. M. Sirunyan et al., CMS Collaboration, Phys. Rev. Lett. **120**, 09230 (2018).
- [44] J. Adam et al., ALICE Collaboration, J. High Energy Phys. **03**, 081 (2016).
- [45] S. Cao, G-Y. Qin, and S. A. Bass, Phys. Rev. **C92**, 024907 (2015).
- [46] A. M. Sirunyan et al., CMS Collaboration, Phys. Rev. Lett. **120**, 202301 (2018).
- [47] V. Greco, C. M. Ko and R. Rapp, Phys. Lett. **B595**, 202 (2004).
- [48] Z. Lin and D. Molnar, Phys. Rev. **C68**, 044901(2003).